Conclusions

The description of TEM propagation on an array of parallel coupled lines in terms of the static capacitance matrix allows a unified treatment of many heretofore seemingly unrelated network configurations. The use of the capacitance matrix transformation provides a simple method, devoid of complicated mathematics, for investigating possible equivalent circuit structures and obtaining new network forms. Furthermore, the techniques described provide considerable physical insight into the meaning of equivalent TEM networks and should be a very useful tool, both computationally and conceptually, to the network designer.

References

[1] R. J. Wenzel, "Exact theory of interdigital band-pass filters and related coupled structures," *IEEE Trans. on Microwave Theory and Techniques*, vol. MTT-13, pp. 559–575, September 1965.
[2] S. O. Rice, "Steady-state solutions of transmission line equations," *Bell Sys. Tech. J.*, vol. 20, pp. 131–178, April 1941.
[3] D. C. Youla, "An introduction to coupled-line network theory," MRI, Polytechnic Institute of Brooklyn, Brooklyn, N. Y., Rept. 960–961, 1961.
[4] E. Ott, "A network approach to the design of multiline 2*N*-port directional couplers," Polytechnic Institute of Brooklyn, Brooklyn, N. Y., Rept. PIBMRI-1236-64; Air Research Development Command, Rome Air Development Center, Griffiss AFB, Rome, N. Y., Contract AF 30(602)-2868, Tech. Rept. RADC-TR-65-41, April 1965.
[5] W. J. Getsinger, "Coupled rectangular bars between parallel plates," *IRE Trans. on Microwave Theory and Techniques*, vol. MTT-10, pp. 65–72, January 1962.
[6] E. G. Cristal, "Coupled circulator cylindrical rods between parallel ground planes," *IEEE Trans. on Microwave Theory and Techniques*, vol. MTT-12, pp. 428–439, July 1964.
[7] R. W. Beatty and D. M. Kerns, "Relationships between different kinds of network parameters, not assuming reciprocity or equality of the waveguide or transmission line characteristic impedances," *Proc. IEEE* (*Correspondence*), vol. 52, p. 84, January 1964.
[8] E. A. Guillemin, *Synthesis of Passive Networks*. New York: Wiley, 1957.
[9] R. M. Fano, L. J. Chu, and R. B. Adler, *Electromagnetic Fields, Energy and Forces*. New York: Wiley, 1960.
[10] E. M. T. Jones and J. T. Bolljahn, "Coupled-strip-transmission-line filters and directional couplers," *IRE Trans. on Microwave Theory and Techniques*, vol. MTT-4, pp. 75–81, April 1956.
[11] S. B. Cohn, "The re-entrant cross section and wide-band 3-dB hybrid couplers," *IEEE Trans. on Microwave Theory and Techniques*, vol. MTT-11, pp. 254–258, July 1963.
[12] R. J. Wenzel and M. C. Horton, "Exact design techniques for microwave TEM filters," Final Rept., U. S. Army Electronics Lab., Fort Monmouth, N. J., 00399(E), Bendix Research Labs., Southfield, Mich., April 1965.
[13] *The Microwave Engineers Handbook and Buyer's Guide*. Brookline, Mass.: Horizon House-Microwave, Inc., 1966, p. 91.
[14] M. C. Horton and R. J. Wenzel, "General theory and design of optimum quarter-wave TEM filters," *IEEE Trans. on Microwave Theory and Techniques*, vol. MTT-13, pp. 316–327, May 1965.
[15] L. Young, "Tables for cascaded homogeneous quarter-wave transformers," *IRE Trans. on Microwave Theory and Techniques*, vol. MTT-9, pp. 233–237, April 1959.

The Design and Construction of Broadband, High-Directivity, 90-Degree Couplers Using Nonuniform Line Techniques

C. P. TRESSELT, MEMBER, IEEE

Abstract—**It is possible, at present, to obtain multioctave bandwidth in symmetrical couplers that employ cascaded quarter-wavelength sections of uniformly coupled line. However, the physical junctions between the various sections contribute reactive discontinuities, which significantly degrade coupler directivity. This paper describes a coupler design employing a continuously tapered coupling coefficient that helps to circumvent the directivity problem.**

Two classes of couplers have been investigated, including one which provides optimum equal-ripple performance. Synthesis has been performed with the aid of both digital and Fourier integral computers. Somewhat tighter center coupling is required in the tapered design to produce bandwidth-mean-coupling-level performance comparable to stepped-coupling design.

Experimental data is presented on several models constructed in three-layer polyolefin stripline.

Manuscript received June 29, 1966; revised August 8, 1966.
The author is with The Bendix Corporation, Research Laboratories Division, Southfield, Mich.

I. Introduction

It is possible to obtain multioctave bandwidth from a single coupler that employs several cascaded quarter-wavelength sections of uniformly coupled line. The use of a symmetric structure guarantees 90° relative phase lead of the coupled port with respect to the transmitted port at all frequencies. Cristal and Young [1] present tables of coupling coefficients required to produce equal-ripple response for the third- through ninth-order designs, and include a comprehensive bibliography covering the historic development of this form of coupler. Tight coupling normally is required in at least one of the sections of a broadband design. This condition has been alleviated to some extent by the application of tandem interconnection [2].

Unfortunately, the spread in coupling values required in adjacent quarter-wave sections, with or without tandem interconnection, is large enough to produce substantial differences in physical line dimensions. The abrupt transition regions between adjacent sections exhibit reactive discontinuities, which degrade coupler directivity, particularly at the higher microwave frequencies. Some compensation for these effects can be achieved by using tuning screws in the junction regions, or, if a dielectric stripline is involved, by using suitably placed capacitive tuning tabs. In general, however, these techniques have not proved very useful above C-band.

This paper describes a design that eliminates the abrupt interconnections between coupled sections. The coupling coefficient is gradually tapered from loose to tight coupling (in the center) and then back to loose in a symmetrical manner to preserve the 90° character of the design. The familiar condition that $\sqrt{Z_{oe} \cdot Z_{oo}} = 1$ must be observed throughout the coupler length to insure that the port adjacent to the transmitted port remains isolated.

Stepped-impedance couplers are, in a sense, a subclass of tapered-line designs. In stepped-impedance devices, coupling is assumed to change abruptly between quarter-wave sections, whereas, in practice, a finite length is required to effect the desired change. The coupling vs. distance characteristic present in a stepped coupler is thus, in effect, tapered. This distinction may be largely neglected for couplers covering UHF and the lower microwave frequencies. However, in multioctave designs covering frequencies through X-band, transition regions take up a significant fraction of coupler length due to the shortness of the quarter-wave sections involved. Consider, for example, the stepped-impedance tandem coupler covering the 1 to 8 GHz band described by Shelton [2]. The transition regions associated with the center quarter-wavelength section of this design take up at least one-third of the center section. The distributed nature of such transitions usually dictates the use of a cut-and-try procedure to determine the best transition shape and location along the axis of the coupler. Misadjustments are readily apparent in the frequency domain since these two transitions provide the largest amplitude Fourier contribution to the overall coupling vs. frequency characteristic [2].

The nonuniform line couplers treated in this paper are tapered gradually enough to permit usage of physical coupling data based on infinitely long, uniformly-coupled line calculations without modification. This has the practical advantage of allowing the geometry of the coupler to be completely specified without the uncertainty associated with the transition regions of stepped coupler designs.

The primary motivation for investigation of tapered-line designs, however, has been the promise of higher directivity. The reactive discontinuities experienced in stepped designs result from nonpropagating higher order modes present in the vicinity of the transitions. While it is true that such evanescent modes will, to some extent, also be excited along the length of the tapered-line geometry, the amplitude of such modes decreases as the taper employed becomes more gradual with respect to wavelength. The equal-ripple tapered-line coupler described in Section IV utilizes essentially a full quarter wavelength to taper between coupling levels for which an abrupt transition is required in the comparable stepped-coupler model. It is unfortunate that directivity is not more amenable to theoretical calculation in either the stepped or tapered cases, the heart of the problem being the lack of a mathematical description for the modes involved in practical line geometries of interest. Experimental comparison is thus indicated and preliminary data on experimental tapered-line couplers is included for this purpose.

II. Analysis of Nonuniform Line Coupler Performance

Generalized coupler theory can be developed with the aid of the transmission line analogy [1]. A nonuniform transmission line is postulated whose characteristic impedance curve equals the even-mode impedance curve of the coupler to be analyzed. Under these conditions, the reflection coefficient of the transmission line is equal in magnitude and phase to the coupled-arm response of the coupler.

The analysis and synthesis of nonuniform line devices is complicated by the fact that exact closed-form solutions have not been developed [3], [4]. Analysis and synthesis can, however, be performed directly by using a loose-coupling approximation. As will be shown later, such results can be modified to cover tighter coupling without resorting to open-form (series) solutions.

Under the assumption of loose coupling, one can show with the aid of the transmission line analogy that coupling C at frequency ω is given by [3]

$$C(\omega) = \int_0^d e^{-2j\omega x/v} p(x) dx \tag{1}$$

where d is the overall coupler length, v is the velocity of propagation in the medium of interest, and

$$p(x) = \frac{1}{2} \frac{d}{dx} \ln Z_{oe}(x). \tag{2}$$

The quantity $p(x)$ is the reflection coefficient distribution which is related by (2) to the even-mode impedance-vs.-distance characteristic of the coupler. The coupling, as given by (1), is the Fourier transform of $p(x)$. Synthesis can thus be performed directly in the first-order approximation by application of an inverse Fourier transformation.

Second-order coupling theory can be obtained with the aid of the transmission line analogy from Youla's equation (66) [4]. The coupler is matched at its input and output so that $\Gamma_g = \Gamma_l = 0$ for the analogous line. Furthermore, the generator and load impedances are equal, so that Youla's equation (66) becomes, in the terminology of this paper,

$$|C(\omega)| = \frac{\left| \int_0^d e^{-j(2\omega x/v)} p(x) dx \right|}{\sqrt{1 + \left| \int_0^d e^{-j(2\omega x)/v} p(x) dx \right|^2}} \cdot \quad (3)$$

A similarity exists between first- and second-order theory, since the same integral expression appears in both solutions. For small values of coupling, the second-order expression reduces to first-order theory. For tighter values of coupling, second-order theory indicates that larger values of $p(x)$ are required for a given coupling level than are indicated by first-order theory. Flat coupling over broad frequency bands is of primary concern. If a $p(x)$ characteristic produces a flat first-order response, the coupling will remain flat in the second-order theory at a lower mean level, as indicated by (3).

Youla [4] presents an exact description of nonuniform line performance in terms of a Volterra integral equation of a type which may always be solved by successive iterations, the resulting series being absolutely and uniformly convergent under broad conditions. The number of iterations required depends on the mean level of coupling and the bandwidth. Unfortunately, a compact synthesis formula corresponding to higher-order theory has not been found.

Further insight into the design problem can be obtained from first-order considerations. Because the even-mode impedance of the coupler is symmetrical about the coupler center, the derivative of the logarithm of this curve will be odd, as shown in Fig. 1(a). It is convenient to shift axis in the first-order integral to take advantage of this fact, obtaining thereby,

$$C(\omega) = -je^{-j(\omega/v)d} \int_{-d/2}^{d/2} \sin 2 \frac{\omega}{v} u \cdot p(u) du \quad (4)$$

where

$$p(u) = \frac{1}{2} \frac{d}{du} \ln Z_{oe}(u). \quad (5)$$

The magnitude and phase of $C(\omega)$, corresponding to $p(u)$ in Fig. 1(a), are shown in Fig. 1(b). By assuming a desired magnitude-vs.-frequency characteristic, and using phase as shown, one can, by inverse Fourier transformation, obtain the required function of coupling vs. distance. A Scientific-Atlanta CF 1 Fourier integral computer has been used to perform this transformation.

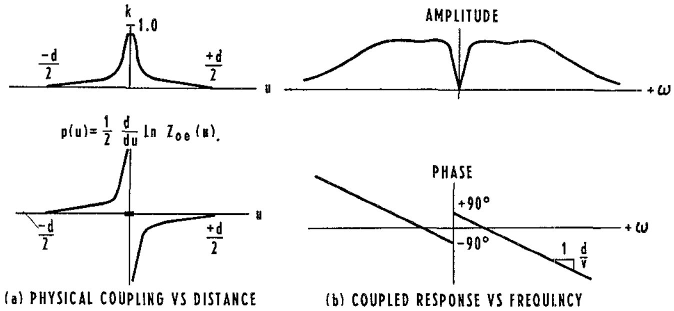

Fig. 1. First-order coupling characteristics.

III. Monotonic $p(u)$ Couplers

The first class of coupler treated possessed a monotonically increasing $p(u)$ characteristic along the length of the coupler, as illustrated in Fig. 1. Pertinent information about the approximation problem for this type of coupler can be obtained by consideration of an impedance-vs.-distance curve that has been found integrable in closed form. Here, it is convenient to use the first-order theory of (4). Let the coupler length d be two units long, and let $p(u)$ be given by

$$p(u) = \frac{-M(1+u)}{2u}, \qquad -1 \le u < 0$$
$$p(u) = \frac{-M(1-u)}{2u}, \qquad 0 < u \le 1. \quad (6)$$

This characteristic is shown in Fig. 2 for $M = 0.201$. The magnitude of $p(u)$ goes to $\pm\infty$ as u approaches zero from either side. Under these conditions, direct substitution of (6) into (4) leads to the result that

$$C(\theta) = jMe^{-j\theta}\left[Si(\theta) + \frac{1}{\theta}(\cos\theta - 1)\right] \quad (7)$$

where

$$\theta = \frac{2\omega}{V} \cdot$$

Response of this coupler for $M = 0.201$ is plotted in Fig. 3(a). The choice of $M = 0.201$ provides a maximum coupling level $C(\theta)_{\max} = 0.3161$, which is -10 dB. Note that coupling rises monotonically with increasing frequency and that coupling is relatively flat for $\theta > 10$.

Equations (5) and (6) require that $Z_{oe} = \infty$ at the coupler center. This is not realizable practically, since the coupling coefficient

$$k(u) = \frac{Z_{oe}^2(u) - 1}{Z_{oe}^2(u) + 1} \quad (8)$$

implies that $k = 1$ at coupler center. Simple truncation of the $p(u)$ characteristic defined by (6) results in a coupling characteristic which droops rather severely with frequency. An iterative technique can be employed

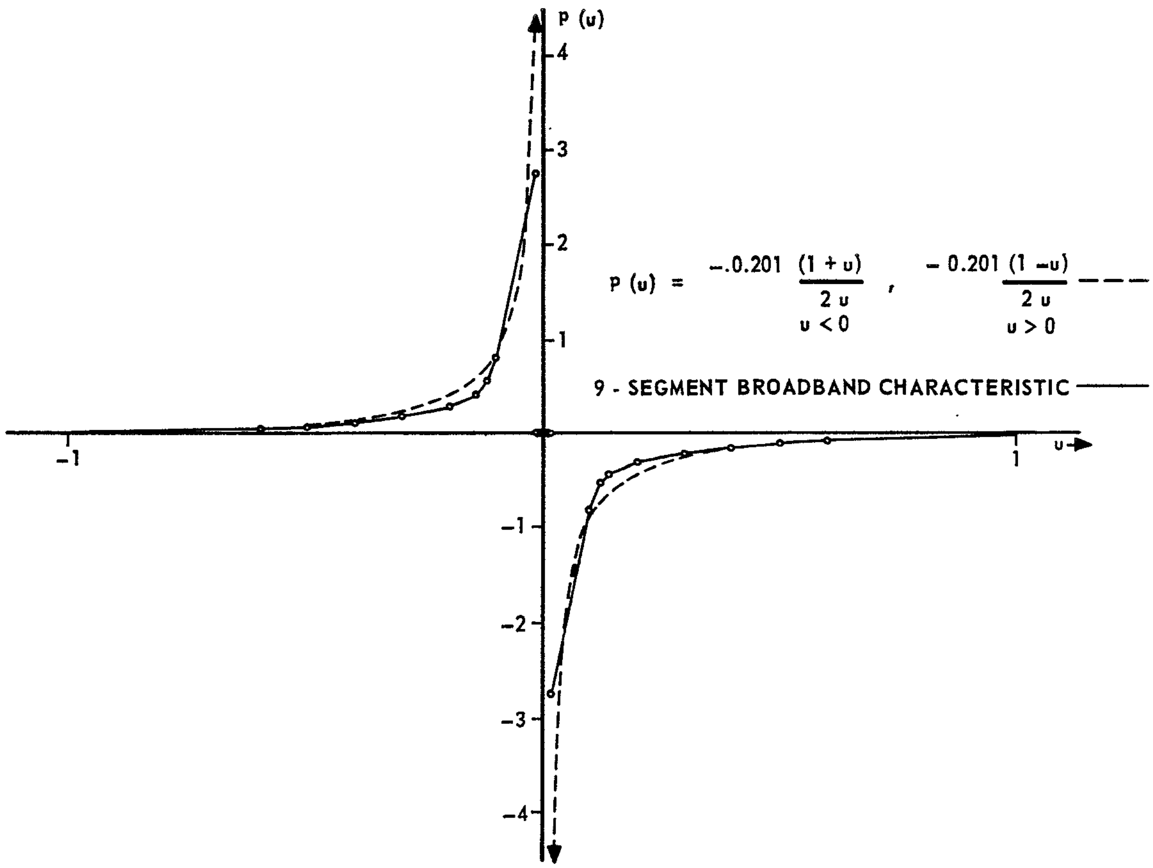

Fig. 2. $p(u)$ vs. u for several monotonic $p(u)$ couplers.

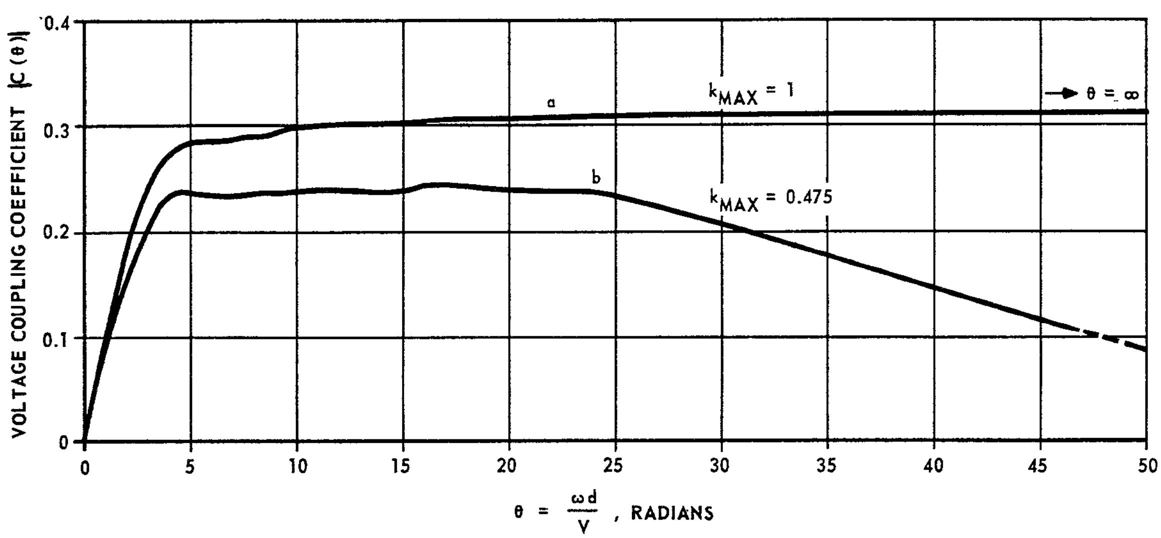

Fig. 3. First-order response of the couplers described in Fig. 2.

to improve such an undesirable response. A curve expressing the difference between a flat coupling level and the given coupler response is formed over the frequency interval in which flat response is desired. Fourier analysis of this error curve will give a set of $p(u)$ values which can be added to the original $p(u)$ characteristic to correct the discrepancy between responses. The response achieved by one particular set of iterations is shown in Fig. 3(b). This characteristic corresponds to the $p(u)$ curve made up of nine straight-line segments shown in Fig. 2. Straight-line segments were used throughout the iterative procedure to minimize the effort required in integrating $p(u)$ to obtain actual coupling coefficients. (A maximum coupling value of $k=0.475$ is required in the center of the coupler.)

One characteristic inherent in the monotonic $p(u)$ type of coupler is the relatively slow dropoff in response at high frequencies. If this response is forced to fall off more rapidly in the correction procedure, a nonmonotonic $p(u)$ function will be produced. The monotonically increasing $p(u)$ coupler was the first tapered design to be investigated because of its relatively smooth coupling characteristic, $k(u)$. This type of coupler is not the most optimum from a mean-coupling bandwidth standpoint as discussed below; however, in moderate bandwidth form, it should prove quite valuable as an instrumentation coupler.

IV. Couplers with Periodic Zeros in $p(u)$

A coupling-vs.-frequency characteristic which would remain flat out to some cutoff frequency, beyond which coupling would rapidly drop to zero, would be highly desirable. All available coupling-bandwidth product would then be employed usefully. One can show, by using first-order coupling theory described earlier in an inverse Fourier transformation sense, that a $p(u)$ distribution given by

$$p(u) = \frac{-1}{\pi} \frac{\sin^2 u/2}{u/2} \tag{9}$$

will provide a first-order mean-coupling level of 1.0 over the frequency range from 0 to 1 radian per second. A 3-dB coupler, then, corresponds to

$$p(u) = \frac{-1}{\pi\sqrt{2}} \frac{\sin^2 u/2}{u/2}.$$

A perfectly flat coupling level would require inclusion of all sidelobes of $p(u)$ from $u=-\infty$ to $+\infty$, and hence would be infinitely long. By truncating $p(u)$ at some point in u, an approximation to the desired coupling can be obtained. The general classification of couplers having periodic zeros in $p(u)$ is based on truncation of (9) which exhibits periodic zeros in the sine function.

The Fourier integral computer was used to investigate the approximation problem. A polar recorder was used on the output to permit plotting several solutions on one sheet for purposes of comparison. A series of five runs was made. The first run used the first positive and first negative lobe of

$$\frac{\sin^2 u/2}{u/2}$$

as a $p(u)$ function. (Positive and negative lobes must be paired together to preserve the symmetric nature of the design.) The next run consisted of the first two positive and first two negative lobes of the same function; more lobes were included, a pair at a time, in subsequent runs. The results are plotted in Fig. 4. As is evident from the figure, the addition of a sidelobe pair increases the number of ripples in the output response by one unit. Also evident from the set of responses is the fact that Gibbs' overshoot is present and does not decrease in amplitude with increasing coupler order (number of sidelobes used).

Ripple level may be equalized by using weighting techniques often employed in antenna array synthesis. The ordinates of symmetrically disposed sidelobes can be weighted with Dolph-Chebyshev coefficients to produce approximate equal-ripple performance. Better results can be obtained by appropriate use of a weighting function derived from the equal-ripple trigonometric polynomials used in the synthesis of stepped-coupler designs. As an example, consider the following digital generated ninth-order polynomial which approximates the constant, unity, in an exact equal-ripple manner (± 5 percent voltage) over the interval $0<\theta\leq\pi$:

$$\begin{aligned} f(\theta) &= 1.2626\sin\theta + 0.3931\sin 3\theta + 0.2049\sin 5\theta \\ &\quad + 0.1170\sin 7\theta + 0.0927\sin 9\theta. \end{aligned} \tag{10}$$

The conventional Fourier representation in the same interval is given by

$$\begin{aligned} g(\theta) = \frac{4}{\pi}\Big(&\sin\theta + \frac{1}{3}\sin 3\theta + \frac{1}{5}\sin 5\theta \\ &+ \frac{1}{7}\sin 7\theta + \frac{1}{9}\sin 9\theta\Big). \end{aligned} \tag{11}$$

Numerical evaluation of $g(\theta)$ will exhibit the usual Gibbs' overshoot phenomenon. The desired weighting function is obtained from that set of coefficients which, when multiplied by the Fourier coefficients in $g(\theta)$, gives the coefficients of the true equal-ripple function $f(\theta)$. Thus

$$\begin{aligned} w_1 &= 1.2626/(4/\pi) = 0.992 \\ w_3 &= 0.3931/(4/3\pi) = 0.929 \\ w_5 &= 0.2049/(4/5\pi) = 0.805 \\ w_7 &= 0.1170/(4/7\pi) = 0.643 \\ w_9 &= 0.0927/(4/9\pi) = 0.656. \end{aligned} \tag{12}$$

The above weighting coefficients, derived from a discrete Fourier series representation of constant coupling, can be applied to the distributed coupling case in the following manner.

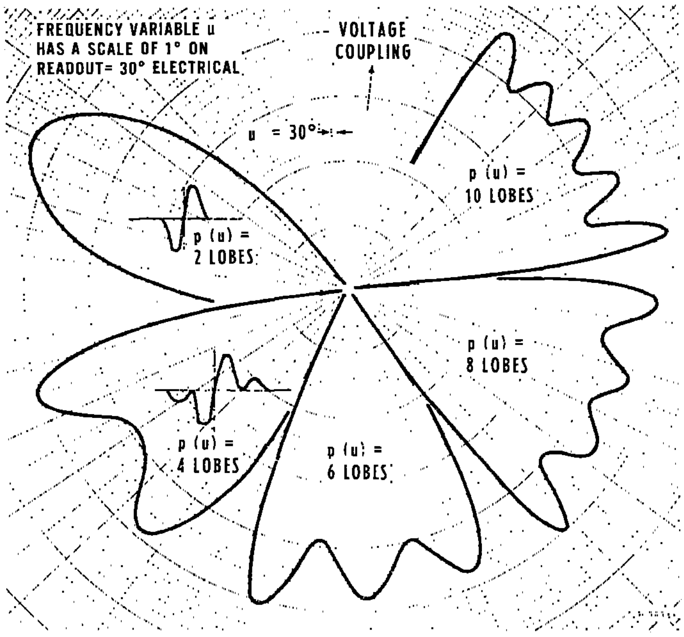

Fig. 4. Frequency response of various truncations of

$$p(u) = \frac{\sin^2 u/2}{u/2}.$$

The first weighting coefficient, w_1, multiplies the ordinates of the first positive and negative lobes of

$$\frac{\sin^2 u/2}{u/2},$$

which extend to $u = \pm 2\pi$. The next coefficient, w_3, multiplies the ordinates of the second set of lobes between $\pm 2\pi$ and $\pm 4\pi$, etc. All five weighting coefficients given in (12) were applied in this manner to the basic $p(u)$ function of (9). The Fourier integral computer was then used to obtain the coupling response.

The resultant coupling is very close to true equal ripple. Because of computer noise, the exact amount of ripple is hard to determine precisely but is about ± 4 percent in voltage. This may be compared with the ± 5 percent voltage ripple associated with the original equal-ripple polynomial from which the weighting function was derived. A more careful analysis using a digital computer to obtain more precision would be desirable. The foregoing weighted $p(u)$ function may be used directly to synthesize various approximate equal-ripple, loose-coupling (first-order) designs.

Couplers designed with the aid of first-order theory, even with exact equal-ripple $p(u)$ data, will not exhibit flat coupling for multioctave bandwidth designs of mean-coupling level greater than about -10 dB. Third-order theory is required as a minimum to describe adequately the effects involved. Fortunately, a closed-form technique, described below, has been found which permits weighting of the $p(u)$ solution to both eliminate Gibbs' overshoot and to include the compensation for tight coupling as required by higher order theory. This technique uses weighting functions derived from exact stepped-coupler designs [1]. Figure 5 indicates approximately a weighted fifth-order $p(u)$ function and the

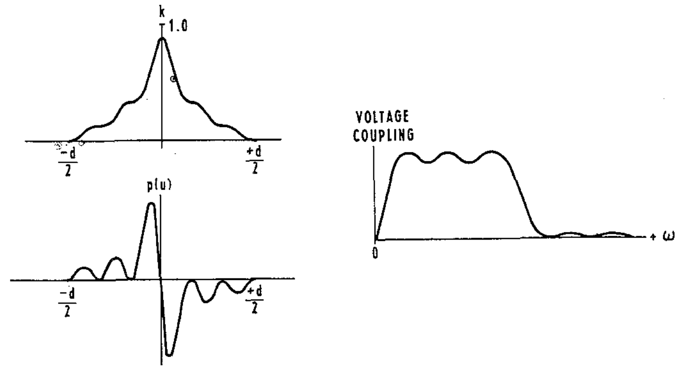

Fig. 5. Response of a typical periodic-zero $p(u)$ coupler.

associated coupling functions in both frequency and distance (k vs. u).

A description of stepped couplers in terms of the

$$p(u) = \frac{1}{2}\frac{d}{du}\ln Z_{oe}(u)$$

domain is required in the process of obtaining the desired weighting function. The coupling coefficients of stepped couplers change discontinuously, so that $p(u)$ consists of a set of Dirac delta functions located periodically with distance, at the discontinuities. The area under each delta function is given by $\frac{1}{2}\ln Z_{i+1}/Z_i$, where Z_i and Z_{i+1} are the even-mode impedances on either side of the discontinuity. Under these conditions, one can show by using (4) that

$$C(\omega) = je^{-j(\omega d/v)} \sum_{n=1}^{(N+1)/2} \ln \frac{Z_{((N+3)/2)-n}}{Z_{((N+1)/2)-n}} \sin (2n-1)\frac{\omega d}{vN} \tag{13}$$

where N is the order of design. (The equal-ripple polynomial listed previously, (10), is of order $N=9$, with $\theta = \omega d/Nv$.)

Cristal and Young's tables [1] give the various even-mode impedances required to build an equal-ripple stepped-coupler for $N=3$, 5, 7, and 9, and for a variety of mean-coupling levels and ripple tolerances. Consider, for example, the case of a stepped ninth-order, 8.34-dB coupler with ripple tolerance of ± 0.30 dB. According to Cristal and Young's tables, such a design exhibits a 10.96:1 bandwidth and consists of the following impedance levels: $Z_1 = 1.031\,34$, $Z_2 = 1.076\,97$, $Z_3 = 1.164\,69$, $Z_4 = 1.357\,71$, $Z_5 = 2.253\,15$. One can form the $p(u)$ plane representation of this coupler by calculating the area under the various delta functions as described previously. Equation (13) thus becomes

$$C(\omega) = je^{-j(\omega d/v)}\left[0.5071 \sin\frac{\omega d}{9v} + 0.1532 \sin\frac{3\omega d}{9v} + 0.0785 \sin\frac{5\omega d}{9v} + 0.0433 \sin\frac{7\omega d}{9v} + 0.0309 \sin\frac{9\omega d}{9v}\right]. \tag{14}$$

The first-order Fourier approximation to 8.34-dB coupling is, from (11),

$$| C(\theta) | = 0.3827\times \frac{4}{\pi}\left|\sin \theta + \frac{1}{3}\sin 3\theta + \frac{1}{5}\sin 5\theta + \frac{1}{7}\sin 7\theta + \frac{1}{9}\sin 9\theta\right| \quad (15)$$

where again the Gibbs' overshoot is present. One obtains the weighting coefficients from a term-by-term comparison of (14) and (15). Thus,

$$\begin{aligned} w_1 &= 0.5071/(0.3827 \times 4/\pi) = 1.040 \\ w_3 &= 0.1532/(0.3827 \times 4/3\pi) = 0.943 \\ w_5 &= 0.0785/(0.3827 \times 4.5\pi) = 0.805 \\ w_7 &= 0.0433/(0.3827 \times 4/7\pi) = 0.623 \\ w_9 &= 0.0309/(0.3827 \times 4/9\pi) = 0.569. \end{aligned} \quad (16)$$

This set of weighting coefficients can be applied to the respective amplitudes of the first five lobe pairs of

$$\frac{\sin^2 u/2}{u/2}$$

to produce equal-ripple results similar to those obtained in weighting the discrete jump solution. It is instructive to compare the weighting coefficients associated with the 8.34-dB coupler, (16), with the weighting coefficients associated with a loose-coupling design, such as given in (12). Both sets of weighting coefficients tend to de-emphasize the higher order terms in order to eliminate Gibbs' overshoot. In the 8.34-dB coupler, however, the lowest term is accentuated because of the tightness of coupling involved. This effect becomes more prominent when 3-dB coupling is desired, in which case, both w_1 and w_2 are typically greater than unity, emphasizing the effect of the higher order theory.

The even-mode characteristic impedance of the distributed coupler can be obtained by a point-by-point integration of the $p(u)$ distribution, as indicated by (5). Fortunately, the integration can be found in tabular form by noting that

$$2\int_0^a \frac{\sin^2 u/2}{u} du = \int_0^a \frac{(1-\cos u)}{u} du = \text{Cin}(a) \quad (17)$$

where Cin is one definition of the cosine integral. The Cin is tabulated in King [5] for arguments through 25. Alternately, one might note that $\text{Cin}(a) = C + \ln a - \text{Ci}(a)$, where $C = 0.5772$ is Euler's constant, and $\text{Ci}(a)$ is an alternate form of cosine integral tabulated in a number of references [6], [7]. The integrand function,

$$2\frac{\sin^2 u/2}{u},$$

has minima every $2\pi n$ radians and has maxima where $\tan u = 2u$. Solutions to the latter equation are tabulated in [8]. For high order sidelobes, the maxima tend to fall halfway between the minima.

The ninth-order solution previously analyzed covers five positive and five negative lobes of the $p(u)$ function, so that the overall coupler length is $d = 20\pi$ units. One can obtain from the Cin tables the area under various positive lobes of the function

$$\frac{\sin^2 u/2}{u/2}.$$

$$\begin{aligned} &\text{1st lobe:} \quad A_1 = 2.438 \\ &\text{2nd lobe:} \quad A_2 = 0.676 \\ &\text{3rd lobe:} \quad A_3 = 0.402 \\ &\text{4th lobe:} \quad A_4 = 0.287 \\ &\text{5th lobe:} \quad A_5 = 0.223. \end{aligned} \quad (18)$$

The weighted area under positive lobes of the ninth-order, 8.34-dB coupler can be determined from (9) by adjusting the mean first-order coupling level to 0.3827 and by applying the appropriate weighting coefficients:

$$\begin{aligned} &\text{1st lobe:} \quad \frac{0.3827}{\pi} \times 2.438 \times 1.040 = 0.3085 \\ &\text{2nd lobe:} \quad \frac{0.3827}{\pi} \times 0.676 \times 0.943 = 0.0776 \\ &\text{3rd lobe:} \quad \frac{0.3827}{\pi} \times 0.402 \times 0.805 = 0.0394 \\ &\text{4th lobe:} \quad \frac{0.3827}{\pi} \times 0.287 \times 0.623 = 0.0218 \\ &\text{5th lobe:} \quad \frac{0.3827}{\pi} \times 0.223 \times 0.569 = \underline{0.0155} \\ &\text{Total Positive Lobe Area} \qquad 0.4628. \end{aligned} \quad (19)$$

The tapered-line coupler can be fabricated from a plot of coupling coefficient vs. distance. This is obtained by first integrating the weighted

$$\frac{\sin^2 u/2}{u/2}$$

function (using the Cin tables [5]) and equating to the integral of

$$p(u) = \frac{1}{2}\frac{d}{du}\ln Z_{oe}(u);$$

that is, $\frac{1}{2}\ln Z_{oe}(u)$. The coupling coefficient, $k(u) = (Z_{oe}^2 - 1)/(Z_{oe}^2 + 1)$, may then be calculated. For example, the maximum value of coupling results from integrating the total positive lobe area so that, from the above data,

$$\tfrac{1}{2}\ln Z_{oe\max} = 0.4628, \text{ from which } Z_{oe\max} = 2.512 \text{ and } k_{\max} = 0.727.$$

The design produced by the procedure outlined above is shown in Fig. 6.

The actual physical length of the coupled region d can be determined once the desired center frequency f_c

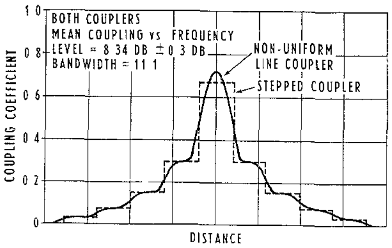

Fig. 6. Comparison of coupling vs. distance characteristics for two classes of coupler design.

of the equal-ripple band has been chosen. It can be shown with the aid of the Fourier integral computer that

$$d = \frac{(N+1)v}{4f_c}. \tag{20}$$

The bandwidth of the tapered-line coupler will be essentially identical to that of the prototype stepped coupler, which, for the example above, is approximately 11:1. If a coupler using this particular taper is to be built to cover 1 to 11 GHz, $f_c = 6 \times 10^9$ Hz. Assuming polyolefin stripline is to be employed, $v = 77.5 \times 10^8$ in/s. Thus,

$$d = \frac{(9+1) \times 77.5 \times 10^8}{4 \times 6 \times 10^9} = 3.23 \text{ inches.}$$

It is interesting to note that (20) states that the equal-ripple tapered-line coupler is exactly one-quarter wavelength longer than the equivalent stepped-impedance coupler.

Figure 6 compares the coupling coefficient for the ninth-order, 8.34 dB, tapered-line design with that of the stepped coupler from which the weighting coefficients were derived. It is evident that the stepped coupler and the tapered-line coupler are related. The tapered-line coupler is about 11 percent longer than the stepped design and requires $k_{max} = 0.727$ in comparison with $k_{max} = 0.672$ for the stepped design. This result is characteristic of the difference between tapered and stepped designs.

The rate of change of coupling with distance is more gradual in the tapered-line design, as is apparent from Fig. 6. Approximately one-quarter wavelength is utilized in tapering between coupling plateaus in the periodic-zero tapered-line model. The abrupt changes in coupling in the corresponding stepped model occur at the center of the tapered regions at the points of maximum rate of change of coupling vs. distance. As mentioned in the Introduction, practical stepped couplers cannot exhibit perfectly abrupt changes in coupling. The present example shows that rather gradual transitions can, in fact, be used while preserving essentially similar response. The chief difference relates to repetitious coupling response at frequencies above the first coupling band: the mathematical model for the ideal stepped coupler repeats at center frequencies which are odd harmonics of the fundamental out to infinite frequency, whereas the periodic-zero tapered-line coupler exhibits essentially zero coupling beyond the first pass band. Practical stepped couplers will exhibit fairly good third harmonic and possibly higher coupling bands if designed for lower frequencies where the transition regions are a small fraction of a quarter wavelength; for higher frequency models, repetition of the second coupling band is typically of poor shape and mean-coupling is lower than the design level showing the presence of appreciable tapering in the physical model.

V. Experimental Models

In reducing to practice the design of couplers having periodic zeros in $p(u)$, a 3-dB coupler was constructed to determine the adequacy of mathematical treatment in predicting mean-coupling level under tight-coupling conditions. Preliminary work on very tight physical coupling indicates that a coupling coefficient of about 0.9 can be achieved in three-layer polyolefin stripline using 0.0015-inch centerboard and 0.062-inch ground plane boards. In this geometry, it is possible to synthesize a tapered-line, 3-dB coupler having more than two-octave bandwidth. The measured response of the coupler is given in Fig. 7. Coupling variation exceeded the design tolerance to ±0.25 dB, primarily because of uncertainty regarding impedances in the stripline geometry. The width of the stripline conductor is approximately one-sixth of that corresponding to $Z_0 = 50$ ohms in the tightly coupled center region (where the thickness of the conductor foil approximately equals the thickness of the dielectric board separating the two lines). The measured isolation on the first trial was, however, a minimum of 21 dB from dc to beyond 7 GHz. The mean coupling of the model was found to be adequately prescribed by the synthesis technique outlined. Broader bandwidth couplers can be obtained by using tandem interconnections of several couplers without resorting to extremely tight coupling levels.

To assure maximum directivity, it is important that the coupler design use fully overlapped coupling in the center to permit crossing of the conductors for purposes of tandem interconnection. A jog in the center caused by overly tight coupling of the lines would defeat the purpose of the tapered-line geometry.

To assure uniform ripple and high isolation, very accurate data on three-layer stripline coupling parameters is necessary. The data employed to date has been obtained from various zero-conductor-thickness, asymptotic solutions. (See, for example, Reference [9].) A 0.010-inch centerboard dielectric thickness, which might typically be used, is small enough in comparison with 1-ounce copper foil (0.0014 inches thick) to cause noticeable deviation from the zero-thickness approximations. In view of the complexity of obtaining useful conformal transformation solutions to the finite conductor-offset stripline problem, an extensive measurement program was initiated to obtain data of the accuracy required. Consequently, a three-layer stripline test fixture

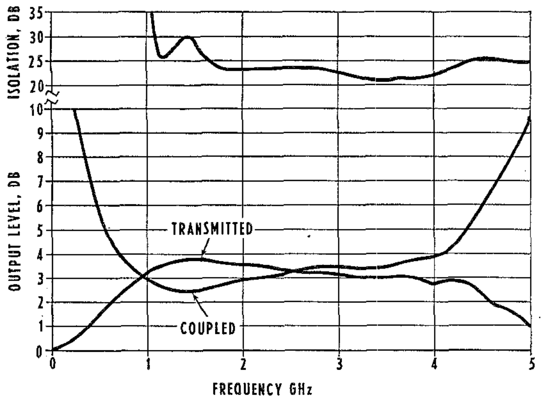

Fig. 7. Measured performance of tapered-line 3-dB coupler having periodic zeros in $p(u)$.

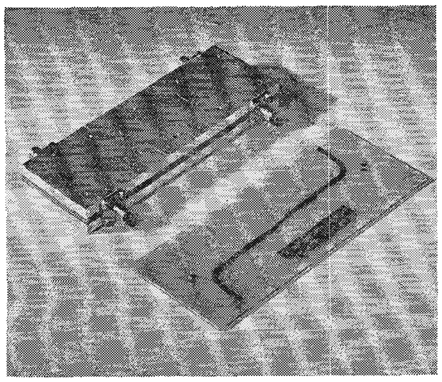

Fig. 8. Ninth-order, 8.34±0.30-dB tapered-line coupler.

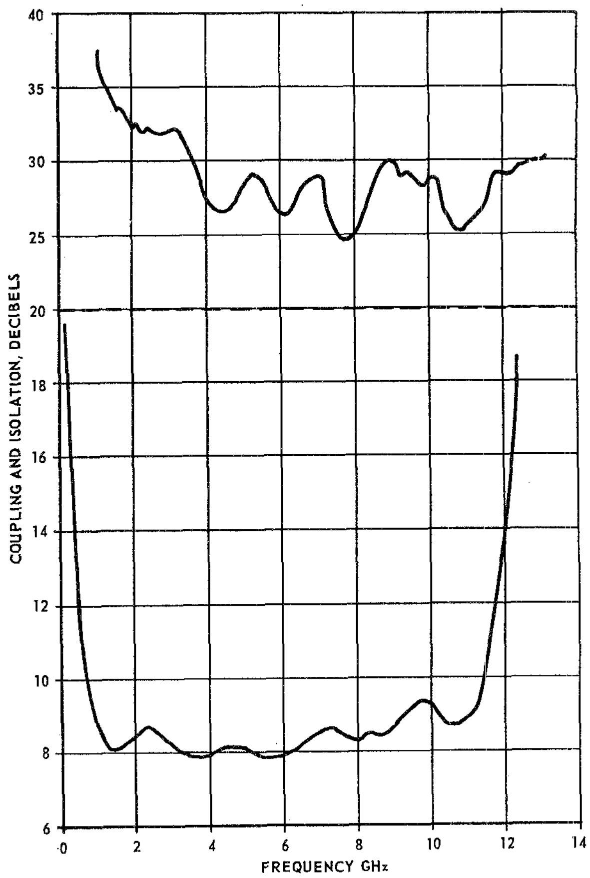

Fig. 9. Measured performance of ninth-order 8.34±0.30-dB tapered-line coupler.

has been constructed recently in which a 6-inch length of uniformly coupled line is measured. A broadband time-domain reflectometer is used to ascertain that overlap has been properly adjusted for a given conductor width to assure that $\sqrt{Z_{oe} \cdot Z_{oo}} = 50$ ohms. Coupling is then measured under matched conditions by both time- and frequency-domain measurements to assure a cross-check of the values obtained. Such a crosscheck has indicated that preliminary measurements made with this fixture are accurate.

Having obtained somewhat more accurate stripline data, the ninth-order, 8.34±0.30-dB coupler described in the preceding section was constructed, as a general verification of the weighting function theory. The maximum required physical coupling coefficient, $k = 0.727$, can be realized in three-layer polyolefin stripline consisting of 0.010-inch shim stock used with 0.062-inch ground-plane boards when the conductors are fully overlapped. The band from 1 to 11 GHz was chosen for realization, requiring an overall coupled line length of 3.24 inches in polyolefin. Figure 8 shows an exterior view of the coupler and an unmounted ground-plane board of the type contained within the case. With careful inspection, the periodic plateaus in the line geometry can be identified. The measured performance of the coupler is shown in Fig. 9. Mean coupling is reasonably close to 8.34 dB, ripple amplitude is of the right order of magnitude, and the number of major ripples, five, corresponds to the order of the design. The deviation of coupling from 8.34 dB toward the high end of the band is attributable partially to an insertion loss of several tenths of a decibel present at the higher frequencies. The foregoing measurements were made every 200 MHz, the curves shown being drawn through each point measured. Low VSWR BRM miniature loads were used in the measurement of isolation; both the generator and the temperature-compensated bolometer detector were well padded with attenuators. The latter padding was found quite desirable in reducing higher order inaccuracy due to multiple reflections. Low VSWR stripline-to-BRM transitions are an integral part of the coupler.

The above coupler showed sensitivity to pressure exerted on the case. This was ultimately traced to the ability of the thin 0.010-inch shim to assume different depths in the region next to the 0.0014-inch thick foil stripline. The isolation shown in Fig. 9 was improved by several decibels with the addition of 1-mil teflon shim stock to the regions around the foil conductors, thereby virtually eliminating the air gap. For best performance, the coupler should be reconstructed using stripline coupling data measured with the extra shim material present (the shim being polyolefin instead of teflon).

The most significant feature of the data given in Figs. 7 and 9 (both tapered couplers) is that isolation is relatively constant over the band and is actually higher at the high-frequency end of the band. The various stripline stepped couplers constructed by the author and those reported on in the literature [2], [10] all exhibit a trend towards decreasing isolation throughout the coupling band, often approaching rather low values at the high frequencies. For example, a 1 to 8 GHz stepped-impedance coupler of 8.34-dB mean level was constructed by the author from data given in Reference [2]. It exhibited isolation within the 1 to 8 operating band which in several narrow bands was at least 10 dB poorer than isolation at any point through 12.5 GHz in the tapered-line model of Fig. 9. The isolation of the tandem interconnection of two such stepped couplers is reported to be 10 dB near 8 GHz [10], which result has been duplicated by the author. Reworking transition regions in these and other stepped couplers to include compensation in the form of capacitive tabs or tuning screws can provide some improvement in isolation over most of the coupling band (excluding the high-frequency region in all cases tried by the author). The tapered-line couplers measured to date provide isolation which remains high through the high-frequency band limit, while completely avoiding the rather laborious trial-and-error process of transition location, shaping, and discontinuity compensation present in stepped-coupler design.

A number of monotonic $p(u)$ couplers have been constructed using approximate stripline impedance data for a 0.010-inch polyolefin shim used between 0.062-inch ground-plane boards. One of the ground-plane boards used in a 7-dB coupler of this variety is shown in Fig. 10. The measured response of this coupler is shown in Fig. 11, along with the normalized first-order description of coupling. The minimum directivity of this coupler is 20 dB up to 7.5 GHz. A tandem coupler composed of two sections similar to the above design has been constructed for use in a phase-to-amplitude antenna processing system which operated successfully through 11 GHz.

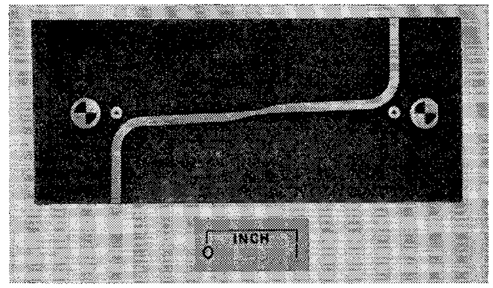

Fig. 10. Stripline board used in 7:1 bandwidth monotonic $p(u)$ coupler.

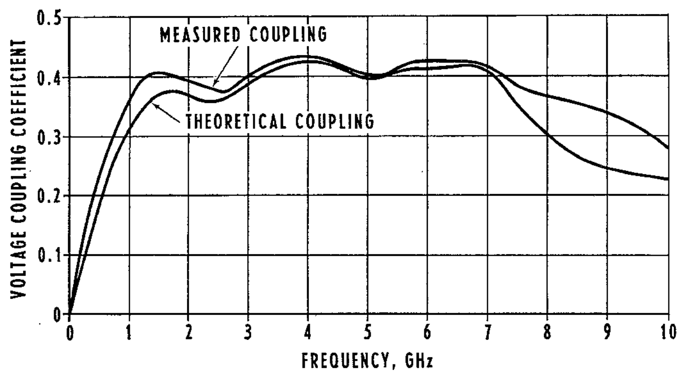

Fig. 11. 7:1 bandwidth monotonic $p(u)$ coupler response.

The limitation on directivity of tapered designs to date has been inaccuracy in knowledge of impedance and coupling of the three-layer stripline configuration. The ultimate limitation on directivity will probably arise from evanescent modes generated in the center of the coupler where the rate of change of line cross section is greatest; the magnitude of this ultimate limit remains to be determined.

VI. Conclusions

Of the two classes of tapered coupler described, monotonic $p(u)$ and periodic-zero $p(u)$, the latter class can be designed to produce approximate equal-ripple coupling performance with the aid of published design tables for stepped-coupling designs. In both types, physical coupling vs. distance varies smoothly throughout the coupled region with promise for realization of high directivity at the higher microwave frequencies. Tapered-line coupler geometry can be completely calculated for the length of the coupler eliminating the trial-and-error procedures often associated with locating, shaping, and compensating transitions between sections in stepped-coupler design. Tapered equal-ripple couplers require an extra quarter wave in overall length and a slightly higher center coupling coefficient to achieve mean coupling-bandwidth performance comparable to that provided by stepped-coupler designs.

References

[1] E. G. Cristal and L. Young, "Theory and tables of optimum symmetrical TEM-mode coupled-transmission line directional couplers," *IEEE Trans. on Microwave Theory and Techniques*, vol. MTT-13, pp. 545–558, September 1965.
[2] J. P. Shelton, R. Van Wagoner, and J. J. Wolfe, "Tandem couplers and phase shifters; a new class of unlimited bandwidth components," presented at the 1964 14th Ann. Symp., USAF Antenna R&D Program, AF Avionics Lab., in cooperation with the University of Illinois, Monticello, Ill., or see *Microwaves*, pp. 14–19, April 1965.
[3] C. B. Sharpe, "An alternative derivation of Orlov's synthesis formula for nonuniform lines," *Proc. IEE* (*London*), vol. 109, Monograph 483E, 1962.
[4] D. C. Youla, "Analysis and synthesis of arbitrarily terminated lossless nonuniform lines," *IEEE Trans. on Circuit Theory*, vol. CT-11, pp. 363–372, September 1964.
[5] R. W. P. King, *The Theory of Linear Antennas.* Cambridge, Mass.: Harvard University Press, 1956, pp. 857–864.
[6] *Tables of Sine, Cosine, and Exponential Integrals*, Table III. Federal Works Admin., Works Progress Admin., N. Y., New York, 1940.
[7] *Handbook of Mathematical Functions*, U. S. Dept. of Commerce, NBS, Appl. Math. Ser. 55. Washington, D. C.: U. S. Govt. Printing Office, June 1964, ch. 5.
[8] *Ibid.*, Table 4.19.
[9] J. P. Shelton, "Impedances of offset parallel-doupled strip transmission lines," *IEEE Trans. on Microwave Theory and Techniques*, vol. MTT-14, pp. 7–15, January 1966.
[10] J. P. Shelton, "Synthesis and design of wideband TEM directional couplers," presented at the 1964 Internat'l Conf. of Microwaves, Circuit Theory, and Information Theory, Tokyo, Japan.